Quasi-Satellite Orbits around Phobos for the Sample Return Mission

By Javier Martín and Simone Centuori[1)]

[1)]*Deimos Space SLU, Spain*

(Received April 6th, 2017)

This paper illustrates the full process of generation of quasi-satellite orbits (QSOs) through a parametric optimization of the initial conditions and control burns, and the selection of the best orbits for observation of the surface of the moons of Mars. QSOs are particular, short-term stable solutions to the three-body problem that can be exploited to remain in close proximity (< 100 km) to the Martian moons for periods in the order of weeks with very low control requirements. In the context of the joint ESA-Roscomos Phobos Sample Return (PhSR) mission, they are used to characterize the surface of the Martian moons Phobos and Deimos, where the dynamical environment is highly perturbed and dominated by the planet to the point that the Hill sphere of Phobos is below its surface at some points. The objective for the trajectory optimization is obtaining a high-resolution image map of both moons with different instruments and, in the case of Phobos, establishing the best landing site for the sampling procedure.

Key Words: Phobos, Quasi-Satellite Orbits, Optimization

Nomenclature

LOF	: local orbital frame
v	: velocity
r	: position
T	: orbital period
w	: QSO amplitude, projection of the relative position on the target's local orbital plane
ω	: angular frequency $= 2\pi T^{-1}$
S/C	: spacecraft
Subscripts	
0	: initial
f	: final
M	: Mars
m	: moon (Phobos/Deimos)

1. Introduction

Phobos Sample Return (PhSR) is a joint ESA-Roscomos mission that aims to characterize Phobos and to collect a sample of its surface to bring back to Earth[1)]. The main science goal of the mission is to understand the formation of the Martian moons Phobos and Deimos and to put constraints on the evolution of the solar system. To do this, samples from Phobos (the moon with the older expected surface) have to be returned to Earth and thus potential landing sites need to be studied beforehand to establish sampling usefulness.

The study of the Phobos surface takes place in a complex dynamical environment that is extremely dominated by Mars: due to the small size of Phobos and its proximity to the planet, even a semblance of Keplerian orbits around the moon is impossible[2)]. Given that the mission needs to return a sample to Earth, the usual mass constraints in space missions are much more stringent due to the need to carry the sampling and return vehicle. Thus, quasi-satellite orbits (QSOs) are used to provide a trajectory that remains in close proximity to the moons and maintains stability in the order of days/weeks, which results in a small number of control burns required during the full observation campaign.

2. Dynamical environment near the moons of Mars

2.1. Physical characteristics

Phobos and Deimos are small bodies, with dimensions in the order of 10 km and markedly non-spherical, see Table 1. They orbit extremely close to Mars, with Phobos even inside the areosynchronous radius: it orbits faster than Mars rotates, so it rises on the west and sets on the east. It is also getting closer to the planet, and will likely end up being torn apart by tidal forces in time scales of tens of millions of years.

Table 1: Physical and orbital characteristics of Phobos and Deimos.

Items	Phobos	Deimos
Ellipsoid axes (km)	13.0x11.4x9.2	7.8x6.0x5.1
GM (km^3/s^2)	$7.07 \cdot 10^{-4}$	$9.62 \cdot 10^{-5}$
Equivalent-vol. radius (km)	11.35	6.25
Semi-major axis (km)	9378	23458
Eccentricity (-)	0.0150	0.0004
Inc. w.r.t. Mars equator (deg)	1.07	0.94
Source (physical data)	Refs.3) and 4)	Refs. 3) and 5)
Source (ephemerides)	JPL MAR097	

Both moons are nearly tidally locked to Mars, although libration motions and small deviations from a perfect long moon axis-planet alignment exist.

2.2. Accelerations near Phobos

The preponderance of Mars in the system is so large that the centre of mass of the system is only a few metres off that of Mars itself – compared to about 4800km for Earth-Moon system. The gravitational parameters of Phobos and Deimos are 8-9 orders of magnitude smaller than that of Mars, which together with the close proximity to the planet makes it impossible to actually *orbit* them in a Keplerian sense.

As an example, Fig. 1 shows the accelerations felt by a test particle on the Mars-Phobos axis, close to the latter. Only at radial distances below 20 km (corresponding to altitudes well below 10 km) does the Phobos gravitational acceleration surpass the Martian tidal term – that is, the Phobos-relative acceleration due to Mars' gravity.

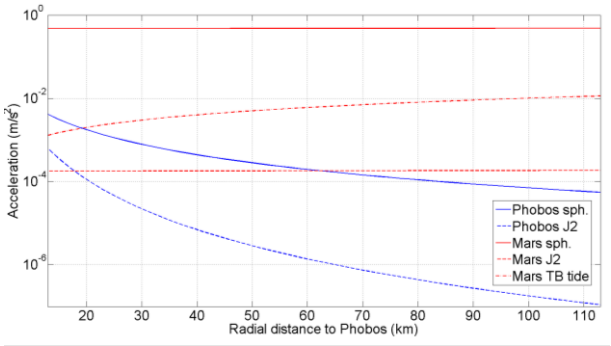

Fig. 1. Gravitational accelerations of Mars and Phobos on a particle on the Mars-Phobos axis. Note that the "Mars TB tide" is the effect of Mars' gravity considered in a Phobos-centred, non-rotating frame.

It seems clear that, for altitudes well over the mentioned ~10 km, it makes more sense to approach the problem from the point of view of co-orbital motion that remains close to the target moon, instead of trying to model a (heavily) perturbed "orbit" around it. The following sections will analyse the problem of relative motion between two co-orbiting objects, starting from the simplified case of rendezvous dynamics and arriving at quasi-satellite orbits.

3. Clohessy-Wiltshire motion

3.1. Dynamics

Considering only two bodies in orbit around a primary ("target" and "chaser" in the literature), the relative motion of the chaser w.r.t. the target can be obtained by writing the dynamics of the chaser in a frame centred at the target. If the target follows a circular orbit, a common choice is a frame where X points towards the target velocity and Z towards the planet, while Y is collinear with the orbital momentum and chosen to follow the right-hand rule. Note that, if the target's orbit is not circular, either the X/V or the Z/R alignment needs to be broken.

The driving force in such a system is likely to be the "gravitational tide" term: the difference of gravitational acceleration between the chaser and the target. In this formulation, the tide caused by a point-mass primary is split off, leaving a differential acceleration $\Delta\gamma$ on the right hand side. This term represents all other influences (e.g. the non-spherical gravity influences, solar radiation pressure, atmospheric drag, thrust commands, etc.). If the distance between the two bodies is small compared to the size of the orbit, the equations can be linearized as follows[6]:

$$\begin{aligned} \ddot{x} - 2\omega\dot{z} &= \Delta\gamma_x \\ \ddot{y} + \omega^2 y &= \Delta\gamma_y \\ \ddot{z} + 2\omega\dot{x} - 3\omega^2 z &= \Delta\gamma_z \end{aligned} \qquad (1)$$

This is commonly described as "rendezvous dynamics", since it was first developed to analyse the rendezvous of a S/C with a target in a circular orbit, like a space station in Earth orbit. Its applicability to the problem of orbits around other small bodies such as comets or asteroids in orbit around the Sun is usually limited, since the gravity of the small body needs to be taken into account from much further away due to the smaller influence of the Sun gravity tide term. However, in the case of Mars, the extreme proximity of the primary makes the equations applicable as a first approximation for orbits that are not too close to the moon.

3.2. Trajectory characteristics

A quick analysis of the equations shows that, in the unperturbed case with $\Delta\gamma = 0$, the out-of-plane motion (the Y direction) is decoupled from the in-plane motion (X-Z). In particular, unperturbed motion in the Y direction is simply an oscillation about the X-Z plane with the same period as the target orbit. This is a positive discovery, since it means that any trajectory that describes a "pseudo-orbit" in the X-Z plane can be modified to have an arbitrary target-relative inclination, thus providing better global observability of the surface.

Focusing on the motion in the X-Z plane, it is readily apparent that there is a family of closed orbits which describe elliptical pseudo-orbits around the target with the same period of the target's orbit around the primary. However, unlike Keplerian orbits, the target is in the centre of the ellipse and not in one of the focal points. The shape of the ellipse is fixed, with the major axis, aligned to the X direction, twice the size of the minor axis. There are no other families of closed orbits in the unperturbed problem.

Including the third dimension once again, three parameters define a closed trajectory: the size of the ellipse, the "inclination" and the phasing between the in-plane and out-of-plane motions, that is, the position of the nodal points on the local orbital plane of the target. The effect of varying these parameters can be seen in Fig. 2, which shows trajectories with a fixed size but varying inclinations, and Fig. 3, which does the same with a fixed inclination but varying phasing parameters. From the figures, it is apparent that the orbits could provide a rather complete coverage for target surface observations.

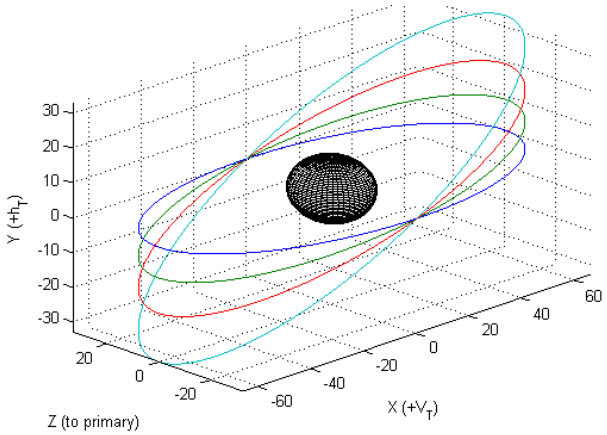

Fig. 2. Closed trajectories in unperturbed Clohessy-Wiltshire motion around a tidally-locked ellipsoidal target, generated with a fixed node on the local orbital plane of the target and varying inclinations 0-45 deg.

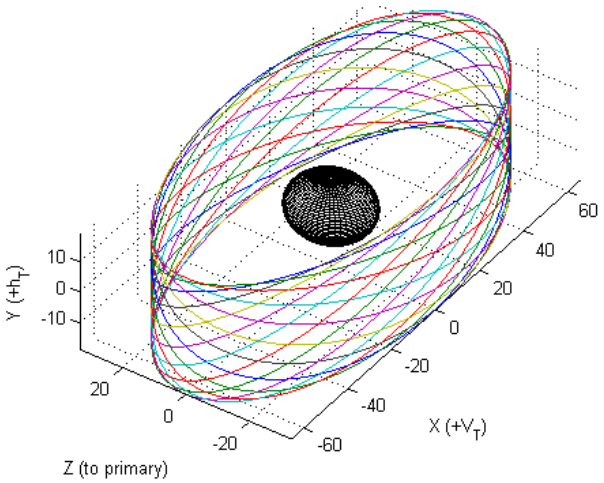

Fig. 3. Closed trajectories in unperturbed Clohessy-Wiltshire motion around a tidally-locked ellipsoidal target, generated with a fixed inclination of 30 deg and varying the in-plane/out-of-plane phase.

It is important to remark, however, that the orientation of the elliptical trajectory in the X-Z plane is fixed, with the largest axis oriented *perpendicular to* the target-primary line. This is a significant disadvantage of this family of trajectories, since a tidally-locked body like the moons of Mars would usually have its largest axis substantially *aligned with* the target-primary line.

Another important concern is that the formulation of the unperturbed C-W motion is disregarding important terms in the acceleration, mainly the gravity of the target itself and the non-sphericity of the primary (especially for Phobos, which is extremely close to Mars). Thus, unperturbed solutions can only be used as an initial guess for the trajectory design and optimization procedure. However, most of these terms could be taken into account if necessary through the $\Delta\gamma$ term, although the applicability of the linearization of the dynamics might be called into question.

Furthermore, as shown in Fig. 1, the influence of the moons falls off rapidly and the effect of Phobos' gravity is overtaken by the Martian tidal term for altitudes over 20 km. Thus, real trajectories are expected to resemble unperturbed C-W closed orbits outside that area of high influence of the moon.

4. Quasi-satellite orbits

4.1. Dynamics

The assumptions used in the generation of quasi-satellite orbits (QSOs) are significantly relaxed from those in C-W dynamics. In particular, the target is not assumed to be in a strictly circular orbit, although the eccentricity is still assumed to be small (as it is in the case of Phobos and Deimos). Thus, the C-W local orbital frame is not well defined, and it is replaced by a VVLH frame – the X axis alignment with target velocity is kept, at the expense of the exact alignment of Z with the target-primary line.

The main difference from a mathematical point of view, however, is that the equations used to propagate the QSOs are not linearized – in order to generate trajectories at a wide range of distances to the target, the full system is used.

Additional perturbations are also introduced, although this is not a fundamental difference, since they could have also been represented in C-W dynamics through the $\Delta\gamma$ term as described above. In the particular case of the PhSR mission, all perturbations were gravitational in nature: from the target moon (either as a point mass or with expansions up to degree and order 3), from the Sun as a third body and from the non-spherical gravity field of Mars.

The expected results vary depending on the distance to the target moon: for close orbits below the limit mentioned in the section above, it is expected that the trajectories become more circular due to the influence of the gravity of the target. On the other hand, for large distances it is expected that trajectories will look significantly like the C-W solutions.

4.2. Design and optimization

The computation of the QSO trajectory is no longer possible through direct symbolic integration. Instead, the obtained orbits are the result of an optimization, in which the initial position is selected with parameters similar to the C-W case and the initial velocity is the optimization variable.

The objective for the optimization is, in abstract terms, the survival and stability of the QSO for a certain amount of time. Several functions to represent this objective were tested, falling in two categories:

- Those that minimize the variation of some function of the moon-relative position, introducing a pressure to make the orbit more circular.
- Those that minimize the variation of that distance at the crossings of a surface of section, thus leaving the distance at other points unconstrained.

In both cases, the function of the position could be either the 3D distance between the S/C and the target moon (the "radius"), or its projection on the local orbital plane of the target (the "amplitude" or *w*). Note that, unlike in the linearized case, there is a coupling between the in-plane and out-of-plane motions.

The initial guess for the optimization variable is the solution to the unperturbed C-W equations. However, for long integration periods >10 T_m, it was observed that behaviour of the orbit was sometimes too unstable for a direct application of the optimization algorithm. In particular, the use of a C-W initial guess did not provide a good enough starting point because the perturbations tended to move the S/C away from the vicinity of the target moon in a few periods, and in some occasions to crash into the moon.

In order to circumvent these problems, a grid-scan step in the initial velocity was introduced before the optimization itself. The result of this strategy can be seen in Fig. 4 for a very close pseudo-orbit, started with 50 deg of target-relative inclination and an initial position of $z_0 = R_m + 20\text{km}$ where R_m is the largest radius of Phobos. Even in a case that is very perturbed by the low altitude and high initial inclination, the grid-scanning algorithm succeeded in finding an initial condition for the optimizer to refine into a trajectory that remained close to Phobos (between 28 and 150 km of central distance) for 30 days without any controls.

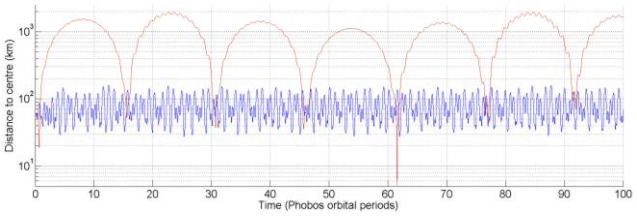

Fig. 4. Results of optimization for a QSO around Phobos, with an initial altitude of 20 km over the largest Phobos radius and an inclination of 50 deg. Red: failure to converge using the initial guess from the C-W solution. Blue: converged trajectory which remains in close proximity to Phobos for at least 100 T_m.

4.3. Trajectory characteristics

The converged trajectories obtained by the above procedure have a shape and properties that matches the behaviour expected by the addition of the mentioned perturbations to the C-W problem. In particular:

- For "distant" orbits, the shape of the orbit is very similar to the unperturbed C-W solution. The main effect of the gravity of the target is a secular variation in the phase between the out-of-plane and the in-plane motions. This is shown in Fig. 5, where a single trajectory close to Phobos sweeps an elliptical cylinder in 20 days – in contrast, the phase is fixed parameter of the orbit in C-W dynamics, as seen in Fig. 2. The projection of the trajectory on the target LOF is very close to a 2:1 ellipse and remarkably stable (see Fig. 6), but the nodal point of the S/C on the local orbital plane of the target precesses as shown on Fig. 7.
- High-inclination orbits are severely destabilized by the same effect. In particular, problems first appear at inclinations over 20-30 deg (depending on the amplitude of the orbit) and worsen progressively.

The resulting trajectories require more intermediate controls to survive for the same time as a similar but less inclined trajectory. The evolution of the distance to the target moon is more unstable even when the trajectory converges; see e.g. the "good" case Fig. 4. As a result, the usage of QSOs with inclinations larger than 50-60 deg was not pursued in the project.

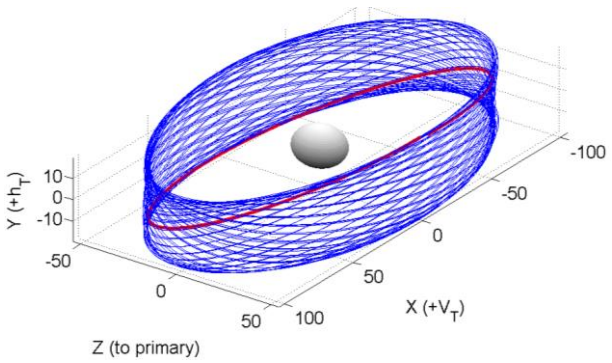

Fig. 5. QSO around Phobos, for a 20-day trajectory case with w_0 = 53 km on the Mars-Phobos line and an inclination of 20 deg. Four intermediate controls were introduced at fixed intervals of 5 days, all below 1.5 cm/s. The first revolution is highlighted.

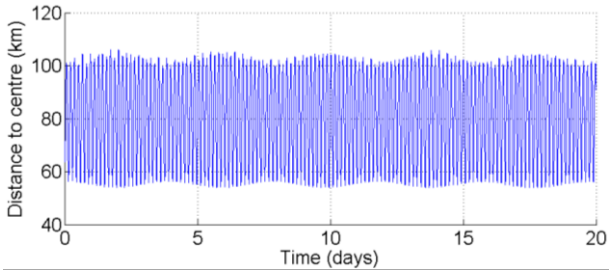

Fig. 6. Instantaneous distance to Phobos in the previous QSO. The envelope is stable, with a superimposed oscillation due to the precession of the node in the local orbital plane of Phobos.

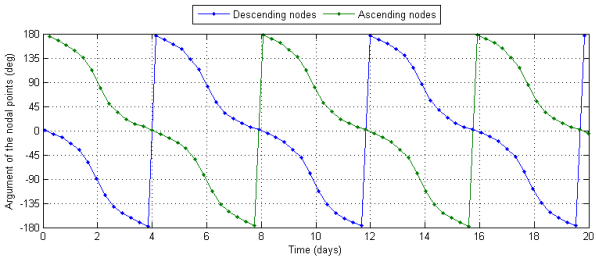

Fig. 7. Argument of the nodal points of the S/C on the Phobos local orbital plane for the previous QSO. Angles are measured from $+V_m$ towards the Mars-pointing direction.

- Finally, orbits very close to the target are even more distorted by its gravity. The projection of the trajectory on the local orbital plane is markedly less elongated, with an axes ratio as low as 1.75:1 for otherwise stable orbits, or even lower values of 1.35:1 for more controlled trajectories. Both cases are represented in in Fig. 8, which contains a 30-day uncontrolled QSO (in blue) and a 20-day trajectory with controls every 5 days (in red).

The change is also very noticeable as a reduction of the pseudo-period (time between two crossings of the YZ plane of the LOF), as can be seen in Fig. 9. In the limit case, if the target was a point mass, the orbit would get more and more circular for lower altitudes, as the gravity of the target started dominating its vicinity.

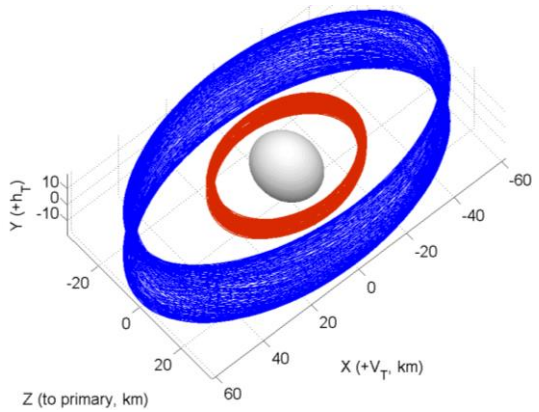

Fig. 8. QSOs in extremely close proximity to Phobos. Blue: 30-day uncontrolled QSO with w_0 = 33 km on the Mars-Phobos line and an inclination of 30 deg. Red: 20-day QSO with controls at 5-day intervals, w_0 = 20 km and an inclination of 15 deg.

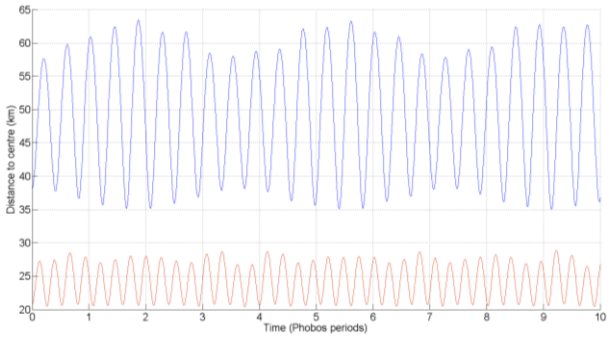

Fig. 9. Instantaneous distance for the previous QSOs, limited to the first ten Phobos periods (around 3.2 days). Notice that the QSO pseudo-periods are shorter than T_m: 83% and 52%, respectively.

5. Application to the Phobos Sample Return project

5.1. Project requirements

In the context of the Phobos Sample Return (PhSR) mission, the scientific requirements[7] describe the study of the shape, structure and composition of the moons of Mars. In particular, this "global characterization phase" requires the measurement of the gravity field and the generation of detailed surface and elevation maps of Phobos and Deimos (although visiting the latter is optional in some mission scenarios) using a variety of instruments in the visible and infrared bands of the spectrum. In the case of Phobos, this phase allows the determination of up to five tentative landing sites that can be further studied in a subsequent local characterization phase.

The specific requirements for the global characterization phase are different for each instrument, and are detailed in Table 2, although the requirements for the IR instruments were invalidated during the project in favour of a redesign with performances similar to the NAC. The resulting surface maps need to cover at least 50% of Phobos and 10% of Deimos, while ensuring that possible landing areas (defined as the latitude band within 20 deg of latitude of the sub-solar point at landing) are fully covered. Other limitations also apply, e.g. the narrow-angle camera can only take images when the solar elevation is between 30 and 60 deg.

Table 2: Phobos surface observation requirements for each instrument.

		NAC	VisNIR	MidIR
Resolution Req.	[m]	3	30	30
Pixel size	[µm]	10	30	25
Image size	[px]	2048	320	315
Field of view	[deg]	1.8	4.6	9
CCD size	[mm]	20	10	8
Focal length	[mm]	652	120	50
Max altitude	[km]	97.78	~~59.75~~	~~30.02~~

Furthermore, indirect observational requirements specify that the coefficients of the gravitational field of Phobos up to degree and order 2 must be measured with a precision of 2%, and its libration around the tidally-locked alignment must be determined within 1%. For Deimos, only the point-mass gravitational parameter must be determined, to 1% precision.

These scientific requirements point to a trajectory for the global characterization phase with a substantial uncontrolled part, allowing the determination of the gravitational and rotational parameters. On the other hand, the surface observation requirements would be better achieved by using trajectories with less or even no variation in the distance to the target moon, in order to have a constant resolution and require less post-processing on the ground side. However, as stated in previous sections, the shape of a QSO is an ellipse with the target at the centre, and whose major axis is aligned to the target velocity, thus nearly perpendicular to the target-primary line for a quasi-circular orbit like that of Phobos or Deimos.

Thus, the summary of trade-offs for the choice of QSOs as for the global characterization phases in PhSR was:

- In favour: QSOs can be generated as long arcs with no controls, leading to a small GNC ΔV cost. This is particularly important given the tight mass constraints.
- In favour: the existence of long periods without controls makes it easier to determine the gravitational and rotational parameters of the moons because it means less thruster noise in the measurements.
- Against: the shape and orientation of the QSO is ill suited for surface imaging, since the obtained data will necessarily have variable resolution. This implies not just that a smaller QSO size will have to be chosen to achieve the resolution requirements, but also that the data obtained will need more post-processing.

All in all, the choice was made in favour of the QSO because of the very tight mass requirements in the mission.

5.2. QSO design and choice

The design and optimization procedure was implemented using a custom toolbox built on top of the open-source Orekit framework. The orbit propagation used a Dormand-Prince integration scheme of order 8(5,3) in local extrapolation mode, although in specific cases this was modified to use a classical Runge-Kutta scheme of order 4 for performance. Due to limitations in Orekit, the dynamics equations were defined and integrated in a non-rotating frame centred at the target.

In order to determine the best QSO for each scenario of the mission, a two-dimensional map in the initial amplitude and inclination was generated, computing one trajectory for each point in the grid and for each scenario, so that the stability and performance of each QSO could be evaluated. The parameters for the generation are described in Table 3, where the initial size parameter is the amplitude w_0 minus the largest spherical radius of the respective moon R_m.

Table 3: Parameters for the generation of the QSO maps.

Parameter	Phobos	Deimos
Initial size parameter [km]	20–50	22–28
Size parameter grid step [km]	2	2
Initial inclination [deg]	40–50	40–50
Inclination grid step [deg]	5	5
Trajectory duration [days]	60	30
Time between controls [days]	30	–

Each trajectory begins at a scenario-specific date on the YZ plane, that is, the initial amplitude is given at the short axis of

the ellipse and the initial nodes are at 0 and 180 deg. The initial guess for the velocity was obtained from a grid-scan algorithm around the C-W solution, as stated earlier. From that result, the optimization was launched with a Nelder-Mead simplex algorithm[9], and the final results were evaluated in terms of the minimum/maximum distance to the target. In a later stage, the performance properties of the solutions in terms of other functions (finer coverage, Earth communication, etc.) were evaluated by other consortium partners, leading to a final trade-off in which a QSO was chosen for each scenario.

5.3. Results: Phobos surface coverage

The stability of each QSO in the map can be observed in Fig. 10 and Fig. 11 in terms of the minimum and maximum distance to the target respectively, before being filtered by observation and communications performance as described above. Note that blank areas represent trajectories that failed to converge to a stable QSO.

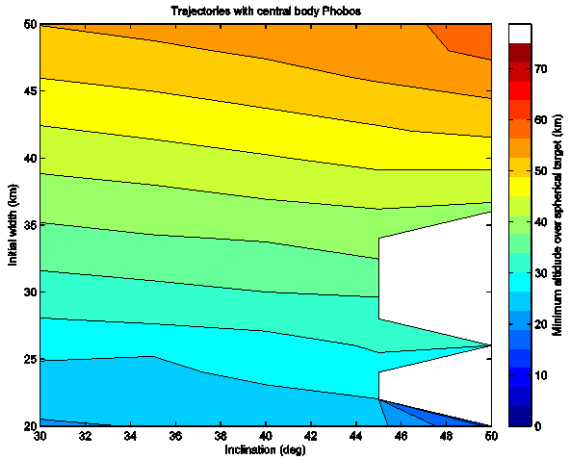

Fig. 10. Minimum distance to Phobos for each QSO in the map for the ESA-standalone scenario of the PhSR mission.

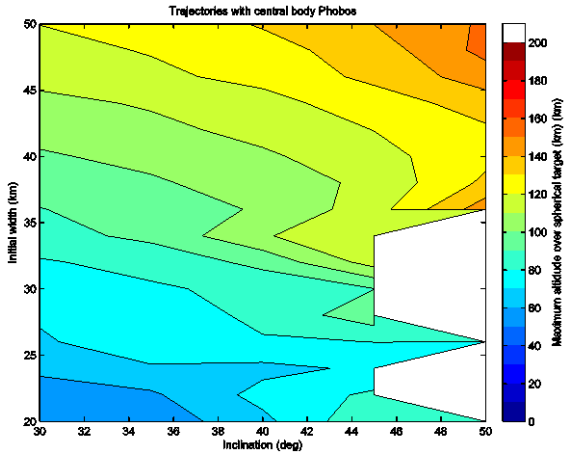

Fig. 11. Maximum distance to Phobos for each QSO in the map for the ESA-standalone scenario of the PhSR mission.

The trajectory that was finally chosen was the same for the ESA-Standalone and the ESA-Roscosmos joint mission scenarios. The trajectory size parameter $(w_0 - R_m)$ is 38 km and the initial inclination is 45 deg, with a single control burn of just 1.2 cm/s. The resulting evolution of the range and solar elevation can be seen in Fig. 12 and Fig. 13, respectively, where the dashed lines show the observability limits of 98 km altitude (a radial distance of 107 km, since in the worst-case the altitude is measured over the *smallest* radius of Phobos) and the 30–60 deg band of solar elevation.

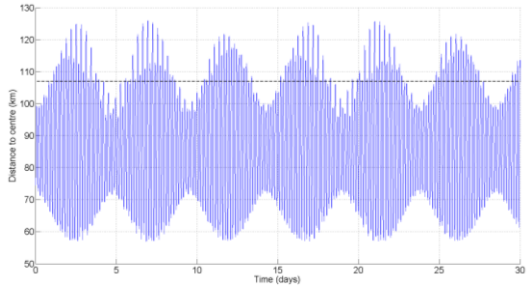

Fig. 12. Instantaneous target range in first 30 days of the Phobos QSO.

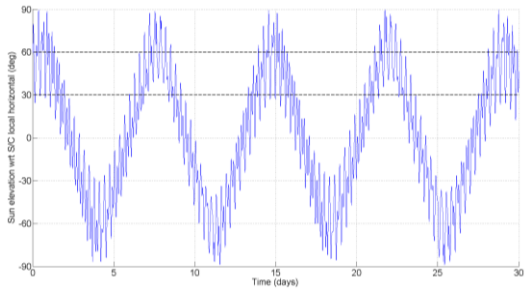

Fig. 13. Instantaneous Sun elevation in first 30 days of the Phobos QSO.

Additionally, the ground track of the S/C was analysed together with the observability limitations in order to verify that the coverage of was adequately distributed in the bands of interest, without leaving zones with a particularly sparse cover. Results are shown in Fig. 14.

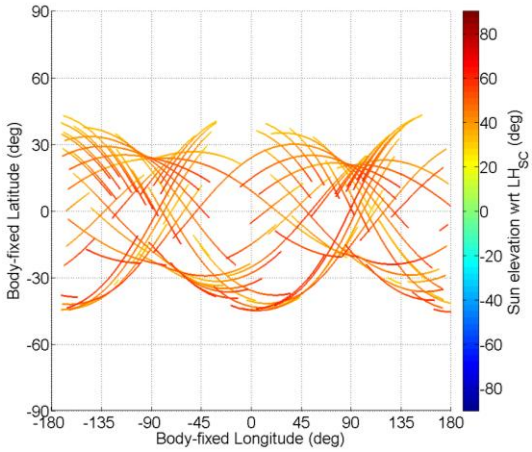

Fig. 14. Ground track of the orbit selected for the global characterization of Phobos, limited to points in which the NAC instrument can operate.

5.4. Results: Deimos surface coverage

The obtained Deimos QSO map is very similar to that of Phobos, but with an important difference: the much larger distance to Mars. The main effect of this change is a slower motion, since the period of Deimos is nearly four times that of Phobos. Since the time allotted for the observation of Deimos is also halved (30 days vs. 60), the total number of revolutions

around Deimos is approximately $^1/_8$ than around Phobos, although this is compensated by the fact that only 10% of the surface needs to be covered per the requirements[7].

On the other hand, orbits near Deimos are inherently more stable due to the weaker perturbing gravity fields, both from the much further primary and the smaller moon. Only one case failed to converge to a valid 30 day ballistic arc.

The orbit finally chosen for the ESA-Roscosmos joint scenario has a size parameter of 38 km and an inclination of 45 deg. As a consequence of the slower motion, the imaging coverage is sparser, as shown in Fig. 15.

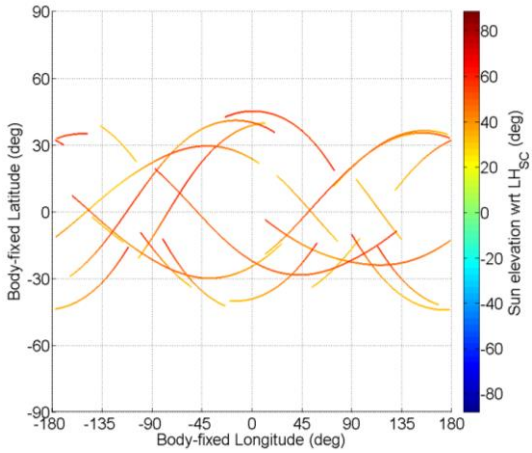

Fig. 15. Ground track of the orbit selected for the observation of Deimos, limited to points in which the NAC instrument can operate.

6. Conclusion

Quasi-satellite orbits can be thought of a particular solution to the three-body problem, or conversely, as a generalization of rendezvous dynamics where the target is massive. Although difficult to generate without a rather precise initial guess, they are an interesting solution for close observation of *small planetary moons* which could not usually be orbited.

The major advantage of QSOs is the high stability of the trajectories, as visible in the uncontrolled 60 and 30-day orbits around Phobos (Fig. 16) and Deimos (Fig. 17). QSOs are able to provide coverage for all longitudes of a tidally-locked body, although the observation distance is necessarily variable.

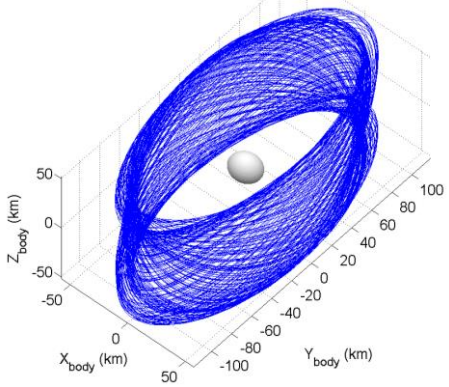

Fig. 16. Plot of the Phobos QSO in the body-fixed frame of the moon.

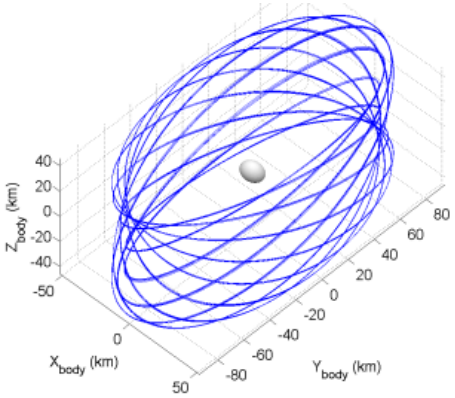

Fig. 17. Plot of the Deimos QSO in the body-fixed frame of the moon.

Acknowledgments

The authors wish to acknowledge the collaboration of other partners in the consortium, including key personnel from Thales Alenia Space, in the coverage and trade-off analysis of the obtained QSO trajectories.

References

1) *Phobos Sample Return phase A study - Mission Requirements Document*, ESA-PSR-ESTEC-MIS-RS-001-i2.0
2) M. Zamaro, J. D. Biggs: *Natural motion around the Martian moon Phobos: the dynamical substitutes of the Libration Point Orbits in an elliptic three-body problem with gravity harmonics*, Celest Mech Dyn Astr DOI 10.1007/s10569-015-9619-2.
3) B. A. Archinal (Chair), M. F. A'Hearn, E. Bowell, A. Conrad, G. J. Consolmagno, R. Courtin, T. Fukushima, D. Hestroffer, J. L. Hilton, G. A. Krasinsky, G. Neumann, J. Oberst, P. K. Seidelmann, P. Stooke, D. J. Tholen, P. C. Thomas, and I. P. Williams (2011). *Report of the IAU Working Group on Cartographic Coordinates and Rotational Elements: 2009*, Cel. Mech. & Dyn. Ast., 109, no. 2, February, 101-135, DOI 10.1007/s10569-010-9320-4
4) N. Borderies and C.F. Yoder: *Phobos' gravity field and its influence on its orbit and physical librations*, Astron. Astrophys. vol. 233, pages 235-251 (1990).
5) D.P. Rubincam, B.F. Chao and P.C. Thomas: *The gravitational field of Deimos*, Icarus vol. 114, pp. 63-67, 1995
6) J.P. Carrou et. al.: *Spaceflight Dynamics*, CNES, ISBN 2-854-28377-5 (1995)
7) *Phobos Sample Return Science Requirements Document*, ESA-SSO-PSR-RS-001_1_2 (2015)
8) E. Hairer, S.P. Norsett, G. Wanner: *Solving Ordinary Differential Equations I (Nonstiff Problems)*, ISBN 3-540-56670-8.
9) J.C. Lagarias, J.A. Reeds, M.H. Wright and P.E. Wright: *Convergence Properties of the Nelder-Mead Simplex Method in Low Dimensions*, SIAM Journal of Optimization, Vol. 9 Number 1, pp.112-147, 1998